

# Targeting CB<sub>2</sub>-GPR55 Receptor Heteromers Modulates Cancer Cell Signaling\*

Received for publication, March 4, 2014, and in revised form, June 17, 2014. Published, JBC Papers in Press, June 18, 2014, DOI 10.1074/jbc.M114.561761

Estefanía Moreno,<sup>a,b,c,1</sup> Clara Andradás,<sup>d,e,1</sup> Mireia Medrano,<sup>a,b,c,1</sup> María M. Caffarel,<sup>d,2</sup> Eduardo Pérez-Gómez,<sup>d,e,3</sup> Sandra Blasco-Benito,<sup>d,e</sup> María Gómez-Cañas,<sup>b,f,g</sup> M. Ruth Pazos,<sup>b,f</sup> Andrew J. Irving,<sup>h</sup> Carme Lluís,<sup>a,b,c</sup> Enric I. Canela,<sup>a,b,c</sup> Javier Fernández-Ruiz,<sup>b,f,g</sup> Manuel Guzmán,<sup>b,d,g</sup> Peter J. McCormick,<sup>a,b,c,i,4</sup> and Cristina Sánchez<sup>d,e,5</sup>

From the <sup>a</sup>Department of Biochemistry and Molecular Biology, University of Barcelona, 08028 Barcelona, Spain, the <sup>b</sup>Centro de Investigación Biomédica en Red de Enfermedades Neurodegenerativas (CIBERNED), 28031 Madrid, Spain, the <sup>c</sup>Institute of Biomedicine of the University of Barcelona, 08028 Barcelona, Spain, the <sup>d</sup>Department of Biochemistry and Molecular Biology I, School of Biology and <sup>e</sup>Department of Biochemistry and Molecular Biology III/Instituto Universitario de Investigación en Neuroquímica, School of Medicine, Complutense University, 28040 Madrid, Spain, the <sup>f</sup>Instituto de Investigación Hospital 12 de Octubre, 28041 Madrid, Spain, the <sup>g</sup>Instituto Ramón y Cajal de Investigación Sanitaria (IRYCIS), Madrid 28034, Spain, the <sup>h</sup>Division of Neuroscience, Ninewells Hospital, University of Dundee, Dundee DD1 9SY, United Kingdom, and the <sup>i</sup>School of Pharmacy, University of East Anglia, Norwich Research Park, Norwich NR4 7TJ, United Kingdom

**Background:** Cannabinoid receptor CB<sub>2</sub> (CB<sub>2</sub>R) and GPR55 are overexpressed in cancer cells and control cell fate.

**Results:** In cancer cells, CB<sub>2</sub>R and GPR55 form heteromers that impact the signaling of each protomer.

**Conclusion:** CB<sub>2</sub>R-GPR55 heteromers drive biphasic signaling responses as opposed to the individual receptors via cross-antagonism.

**Significance:** These heteromers may explain some of the biphasic effects of cannabinoids and, therefore, constitute potential new targets in oncology.

The G protein-coupled receptors CB<sub>2</sub> (CB<sub>2</sub>R) and GPR55 are overexpressed in cancer cells and human tumors. Because a modulation of GPR55 activity by cannabinoids has been suggested, we analyzed whether this receptor participates in cannabinoid effects on cancer cells. Here we show that CB<sub>2</sub>R and GPR55 form heteromers in cancer cells, that these structures possess unique signaling properties, and that modulation of these heteromers can modify the antitumoral activity of cannabinoids *in vivo*. These findings unveil the existence of previously unknown signaling platforms that help explain the complex behavior of cannabinoids and may constitute new targets for therapeutic intervention in oncology.

G protein-coupled receptors participate in the control of many different physiological processes, and their deregulation contributes to numerous human diseases (1, 2). Two decades

ago, cannabinoid receptor type 1 (CB<sub>1</sub>R)<sup>6</sup> and type 2 (CB<sub>2</sub>R) were identified and cloned (3). They are part of the endocannabinoid system, which consists at least of these two receptors, their endogenous ligands (the endocannabinoids), and the enzymes that produce and metabolize these signaling lipids (3). This system modulates a wide variety of physiological functions, including cell fate (3, 4). Therefore, it has been described that cannabinoids, in most cases via CB<sub>1</sub>R and/or CB<sub>2</sub>R, direct cells toward proliferation, differentiation, or death, depending on the cell type and its specific context (5). In tumor cells in particular, these compounds usually produce proliferation-inhibiting and death-inducing effects both *in vitro* and *in vivo* (6), making them promising therapeutic options for the management of cancer. More recently, another G protein-coupled receptor, G protein-coupled receptor 55 (GPR55), has been related to cannabinoids (7). In this case, the pharmacology of the receptor is controversial, and, although some authors have reported cannabinoid actions via GPR55, to date, this receptor does not formally belong to the cannabinoid receptor family (8). Several publications support that lysophosphatidylinositol (LPI), another signaling lipid, is a putative GPR55 endogenous ligand (9, 10). Like its close relatives CB<sub>1</sub>R and CB<sub>2</sub>R, GPR55 has been implicated in the control of cancer cell fate (11). Specifically, this receptor promotes cancer cell proliferation both in cell cultures and in animal models of cancer (12–14). However, the mechanistic details behind these effects remain

\* This work was supported by Spanish Ministry of Economy and Competitiveness Grant PI11/00295 (to C. S.), by a Ramón y Cajal fellowship (to P. J. M.), by Madrid Regional Government Grant S2010/BMD-2308 (to M. G.), and by funds from TV3 Marató Project 308/C/2013 (to P. J. M.).

<sup>1</sup> These authors contributed equally to this work.

<sup>2</sup> Present address: Department of Pathology, University of Cambridge, Cambridge, CB2 1QP, United Kingdom.

<sup>3</sup> Recipient of a postdoctoral research contract from the Fundación Científica Asociación Española Contra el Cáncer.

<sup>4</sup> To whom correspondence may be addressed: School of Pharmacy, CP 1.44, University of East Anglia, Norwich Research Park, Norwich NR4 7TJ, United Kingdom. Tel.: 44-1603-597197; E-mail: p.mccormick@uea.ac.uk.

<sup>5</sup> To whom correspondence may be addressed: Dept. of Biochemistry and Molecular Biology I, School of Biology, Complutense University, C/José Antonio Novais, 2, 28040 Madrid, Spain. Tel.: 34-913944668; Fax: 34-913944672; E-mail: cristina.sanchez@quim.ucm.es.

<sup>6</sup> The abbreviations used are: CB<sub>1</sub>R, type 1 cannabinoid receptor; CB<sub>2</sub>R, type 2 cannabinoid receptor; LPI, lysophosphatidylinositol; BRET, bioluminescence resonance energy transfer; Rluc, *Renilla* luciferase; PLA, proximity ligation assay; DMR, dynamic mass redistribution; THC,  $\Delta^9$ -tetrahydrocannabinol; PTX, pertussis toxin; CTX, cholera toxin; HBA, 4-[4-(3-hydroxyphenyl)-3-(4-methylphenyl)-6-oxo-1H,4H,5H,6H-pyrrolo[3,4-c]pyrazol-5-yl]benzoic acid; FK, forskolin; ANOVA, analysis of variance.

unclear, in part because of the lack of clarity regarding the pharmacology of the receptor.

The classical pharmacological paradigm associating one ligand with one receptor and one receptor with one signaling pathway is being replaced with the view that G protein-coupled receptor-receptor interactions are an important mechanism that can modulate the pharmacological properties of each protomer (15). Here we aimed to determine whether CB<sub>2</sub>R and GPR55, two receptors that are overexpressed in most human tumors and control cancer cell fate (6, 12, 13), can form heteromers in cancer cells and, if so, whether these complexes might play a role in cannabinoid signaling in tumors.

## EXPERIMENTAL PROCEDURES

**Cells, Cell Cultures, and Transfections**—HEK293 AD cells stably expressing CB<sub>2</sub>R (HEK-CB<sub>2</sub>) or HA-GPR55 (HEK-GPR55) or coexpressing both receptors (HEK-CB<sub>2</sub>-GPR55) were developed as described previously (16, 17). All HEK293-derived cells were grown in DMEM (Invitrogen) supplemented with 2 mM L-glutamine, 100 μg/ml sodium pyruvate, 100 units/ml penicillin/streptomycin, minimal essential medium non-essential amino acid solution (1/100), and 10% (v/v) heat-inactivated FBS (Invitrogen) in the presence of the corresponding selection antibiotic (0.2 mg/ml of zeocin for HEK-CB<sub>2</sub> cells, 0.3 mg/ml of G418 for HEK-GPR55 cells, or 0.2 mg/ml of zeocin and 0.3 mg/ml of G418 for HEK-CB<sub>2</sub>-GPR55 cells). BT474 human breast adenocarcinoma cells endogenously expressing CB<sub>2</sub>R and GPR55<sup>7</sup> or stably transfected with a 3×HA-GPR55 construct (BT474-GPR55) and selected by FACS were maintained in RPMI medium supplemented with 10% FBS, penicillin/streptomycin, and 0.4 mg/ml G418. Human glioblastoma T98G cells endogenously expressing CB<sub>2</sub>R and GPR55 (at similar levels as BT474 cells)<sup>7</sup> or stably transfected with selective CB<sub>2</sub>R or GPR55 shRNAs (Genecopoeia, Rockville, MD) and selected by FACS were grown in DMEM supplemented with 2 mM L-glutamine, 100 μg/ml sodium pyruvate, 100 units/ml penicillin/streptomycin, minimal essential medium non-essential amino acid solution (1/100), and 10% (v/v) heat-inactivated FBS in the presence of the corresponding selection antibiotic (5 μg/ml puromycin for T98G-shGPR55 and T98G-shCB<sub>2</sub>). For transient transfections, HEK293 and BT474 cells were transfected with the corresponding fusion protein cDNA by the PEI (Sigma) method (18).

**Bioluminescence Resonance Energy Transfer (BRET)**—For BRET, GPR55-RLuc, CB<sub>2</sub>R-YFP, and Ghrelin 1a receptor-YFP fusion proteins were obtained as follows. The human cDNAs for CB<sub>2</sub>R, GPR55, or the Ghrelin 1a receptor were cloned into pcDNA3.1 and amplified without their stop codons using sense and antisense primers harboring unique EcoRI and BamHI sites for CB<sub>2</sub>R or the ghrelin receptor or harboring HindIII and BamHI for GPR55. The amplified fragments were subcloned to be in-frame with *Renilla* luciferase (RLuc) into the EcoRI and BamHI restriction sites of the pcDNA3.1-RLuc vector (pRLuc-

N1, PerkinElmer Life Sciences) or the pEYFP-N1 vector (enhanced yellow variant of GFP, Clontech, Heidelberg, Germany) to generate the plasmids that express proteins fused to RLuc or YFP on the C-terminal end (GPR55-RLuc, CB<sub>2</sub>R-YFP, and Ghrelin 1a receptor-YFP). The expression of the constructs was tested as described previously (19). HEK293 or BT474 cells were transiently cotransfected with a constant amount of cDNA encoding for proteins fused to RLuc as a BRET donor and with increasing amounts of the cDNA corresponding to proteins fused to YFP as a BRET acceptor. The fusion protein expression and BRET values were quantified as described previously (20) using a Mithras LB 940 that allows the integration of the signals detected in the short wavelength filter at 485 nm (440–500 nm) and the long wavelength filter at 530 nm (510–590 nm) (20). The net BRET is defined as [(long wavelength emission)/(short wavelength emission)] – Cf, where Cf corresponds to [(long wavelength emission)/(short wavelength emission)] for the donor construct expressed alone in the same experiment. Data were fitted to a non-linear regression equation, assuming a single phase saturation curve with GraphPad Prism software (GraphPad, San Diego, CA). BRET is expressed as milliBRET units (net BRET × 1000). In saturation curves, the relative amount of BRET is given as a function of 100 × the ratio between the fluorescence of the acceptor (YFP) and the luciferase activity of the donor (RLuc).

**In Situ Proximity Ligation Assays (PLA)**—Cells were grown on glass coverslips and fixed in 4% paraformaldehyde, washed with PBS containing 20 mM glycine, permeabilized with the same buffer containing 0.05% Triton X-100, and washed successively with PBS. CB<sub>2</sub>R-GPR55 heteromers were detected using the Duolink II *in situ* PLA detection kit (Olink, Bioscience, Uppsala, Sweden). After 1 h of incubation at 37°C with the blocking solution in a preheated humidity chamber, cells were incubated overnight in the antibody dilution medium with a mixture of equal amounts of mouse anti-HA antibody (1:100, Sigma) or rabbit anti-GPR55 antibody (1:100, Abcam, Cambridge, UK) coupled directly to a DNA minus chain to detect HA-GPR55 or endogenous GPR55 and rabbit anti-CB<sub>2</sub>R antibody (1:100, Cayman Chemical, Ann Arbor, MI) coupled directly to a DNA plus chain. Cells were washed with wash buffer A at room temperature and incubated in a preheated humidity chamber for 30 min at 37°C with the ligation solution (Duolink II ligation stock, 1:5, and Duolink II ligase, 1:40) to induce annealing and ligation of the two DNA probes. Amplification was done with the Duolink II detection reagents red kit, which contains fluorescence nucleotides. After exhaustive washing at room temperature with wash buffer B, cells were mounted using mounting medium with DAPI. The samples were observed under a Leica SP2 confocal microscope (Leica Microsystems, Mannheim, Germany). Red fluorescent images were processed with ImageJ software. PLA requires that both receptors be close enough to allow the two different antibody-DNA probes to be able to ligate (<17 nm) (21, 22). If the receptors are within sufficient proximity, a punctate fluorescent signal can be detected by confocal microscopy.

**Dynamic Mass Redistribution (DMR) Assays**—The agonist-induced cell global signaling signature was determined by label-free technology measuring the DMR using an EnSpire® multi-

<sup>7</sup> E. Moreno, C. Andradás, M. Medrano, M. M. Caffarel, E. Pérez-Gómez, S. Blasco-Benito, M. Gómez-Cañas, M. R. Pazos, A. J. Irving, C. Lluís, E. I. Canela, J. Fernández-Ruiz, M. Guzmán, P. J. McCormick, and C. Sánchez, unpublished data.

mode plate reader (PerkinElmer Life Sciences) (23). Refractive waveguide grating optical biosensors, integrated in 384-well microplates, allowed measurements of changes in local optical density in a detection zone up to 150 nm above the surface of the sensor. Cellular mass movements induced upon receptor activation were detected by illuminating the underside of the biosensor with polychromatic light and measured as changes in wavelength of the reflected monochromatic light that is a function of the index of refraction. The magnitude of this wavelength shift (in picometers) is directly proportional to the amount of cell movement. Briefly, 24 h before the assay, cells (10,000 cells/well) were seeded in 384-well sensor microplates and cultured to obtain 70–80% confluent monolayers. Before the assay, cells were washed twice with assay buffer (Hanks' balanced salt solution with 20 mM HEPES (pH 7.15)) and incubated for 2 h in assay buffer with 0.1% dimethyl sulfoxide in the reader at 24 °C. Thereafter, the sensor plate was scanned, and a baseline optical signature was recorded before adding the test compounds dissolved in assay buffer containing 0.1% dimethyl sulfoxide. DMR responses were monitored for at least 2000 s. Kinetic results were analyzed using EnSpire workstation software version 4.10.

**cAMP Production**—Homogeneous time-resolved (TR) fluorescence energy transfer (FRET) assays were performed using the Lance Ultra cAMP kit (PerkinElmer Life Sciences) on the basis of the competitive displacement of a europium chelate-labeled cAMP tracer bound to a specific antibody conjugated to acceptor beads. We first established the optimal cell density for an appropriate fluorescent signal. This was done by measuring the TR-FRET signal, determined as a function of forskolin concentration using different cell densities. The forskolin dose-response curves were related to the cAMP standard curve to establish which cell density provides a response that covers most of the dynamic range of the cAMP standard curve. Cells (1000 cells/well) were pretreated with the antagonists or the corresponding vehicle (dimethyl sulfoxide) in white ProxiPlate 384-well microplates (PerkinElmer Life Sciences) at 25 °C for 20 min and stimulated with agonists for 15 min before adding 0.5  $\mu$ M forskolin or vehicle and incubating for an additional 15-min period. Fluorescence at 665 nm was analyzed on a PHERAstar Flagship microplate reader equipped with a homogeneous time-resolved fluorescence energy transfer optical module (BMG Lab Technologies, Offenburg, Germany).

**ERK-1/2 Phosphorylation**—Cells (35,000 cells/well) seeded in 96-well poly-D-lysine-coated plates (Sigma-Aldrich) were pretreated at 25 °C for 20 min with the antagonists and stimulated for an additional 7 min with the indicated agonists. Phosphorylation was determined in white ProxiPlate 384-well microplates (PerkinElmer Life Sciences) by  $\alpha$ -screen bead-based technology using the amplified luminescent proximity homogeneous assay kit (PerkinElmer Life Sciences) and the EnSpire multimode plate reader (PerkinElmer Life Sciences). Phosphorylation is expressed in arbitrary units, ALPHA counts, as measured by light emission at 520–620 nm by the acceptor beads. To evaluate phospho-ERK-1/2 expression in tumors, a Western blot analysis was performed. Tumor lysates were subjected to SDS-PAGE, and proteins were transferred onto polyvinylidene fluoride membranes. Blots were incubated with anti-

phospho-ERK (Thr-202/Tyr-204), anti-ERK (Cell Signaling Technology, Danvers, MA), and anti- $\alpha$ -tubulin (Sigma-Aldrich) antibodies. Luminograms were obtained with the Amersham Biosciences enhanced chemiluminescence detection kit (GE Healthcare), and the densitometric analysis was performed with Quantity One software (Bio-Rad).

**[<sup>35</sup>S]GTP $\gamma$ S Binding Assays**—HEK-GPR55 cells were rinsed twice in phosphate-buffered saline, detached from dishes by incubation with a buffer containing 5.6 mM glucose, 5 mM KCl, 5 mM HEPES, 137 mM NaCl, and 1 mM EGTA (pH 7.4), and collected by centrifugation (500  $\times$  g) at 4 °C. The pellets were then resuspended in ice-cold lysis buffer (0.2 mM MgSO<sub>4</sub>, 0.38 mM KH<sub>2</sub>PO<sub>4</sub>, 0.61 mM Na<sub>2</sub>HPO<sub>4</sub>, and 0.5% PMSF (pH 7.4)) and homogenized by vortexing. HEK-GPR55 membranes were isolated by centrifugation (20,000  $\times$  g for 20 min), and pellets were resuspended in 50 mM Tris-HCl buffer (pH 7.4). Protein concentration was determined by detergent compatible protein assay kit (Bio-Rad). Membranes were stored at –80 °C until used for analysis of LPI-induced stimulation of [<sup>35</sup>S]GTP $\gamma$ S binding. For this analysis, we followed a procedure published previously (24) in which cell membranes (20  $\mu$ g of protein/ml) were incubated for 120 min at 30 °C in assay buffer (100 mM NaCl, 50 mM Tris-HCl, 10 mM MgCl<sub>2</sub>, 1 mM EGTA, 1 mM DTT, 50  $\mu$ M GDP, and 1 mg/ml BSA (pH 7.4)) containing 0.1 nM [<sup>35</sup>S]GTP $\gamma$ S and increasing concentrations of LPI (10<sup>–10</sup>–10<sup>–5</sup> M) in the presence or absence of 10<sup>–6</sup> M  $\Delta^9$ -tetrahydrocannabinol (THC, The Health Concept, Richelbach, Germany). Non-specific binding was determined in the presence of 10  $\mu$ M unlabeled GTP $\gamma$ S. Reactions were terminated by rapid filtration performed by a Harvester Filtermate (PerkinElmer) with Filtermate A GF/C filters. Filters were rinsed nine times with washing buffer (50 mM Tris-HCl and 1 mg/ml BSA (pH 7.4)) and left to dry, and melt-on scintillation pads (Meltilex A, Perkin Elmer Life Sciences) were melted onto them. The bound radioactivity was quantified by a liquid scintillation spectrophotometer (Wallac MicroBeta Trilux, PerkinElmer Life Sciences). Results were normalized as percent change over basal level (set at 100%) and corresponded to three separate experiments, each performed in triplicate. Data were analyzed by nonlinear regression analysis of sigmoidal dose-response curves using GraphPad Prism 5.01.

**Tumor Generation and Animal Treatments**—Tumors were induced in 6-week-old athymic male mice (n = 6/experimental group; Harlan Interfauna Iberica, Barcelona, Spain) by subcutaneous injection of 10  $\times$  10<sup>6</sup> T98G human glioblastoma cells in PBS supplemented with 0.1% glucose. Half of the animals were treated with double-stranded RNA duplexes for human GPR55 (ON-TARGETplus SMARTpools) from Dharmacon-Thermo Scientific (Lafayette, CO). The sequences were 5'-GAAUCCGCAUGAACAUCAUU-3', 5'-GAGAAACAGCUUUAUCGUAAUU-3', 5'-AAGAACAGGUGGCCCGAUUUU-3', and 5'-GCUACUACUUUGUCAUCAAUU-3'. The other half was treated with a non-targeted control siRNA from Applied Biosystems-Ambion (Austin, TX). The sequence was 5'-UUCUCCGAACGUGUCACGUtt-3'. siRNA was mixed with AteloGene (Koken, Tokyo, Japan) and injected locally when tumors reached approximately 200 mm<sup>3</sup> (day 1) and on day 7. At the same time, each group was treated peritumorally with THC (1.5



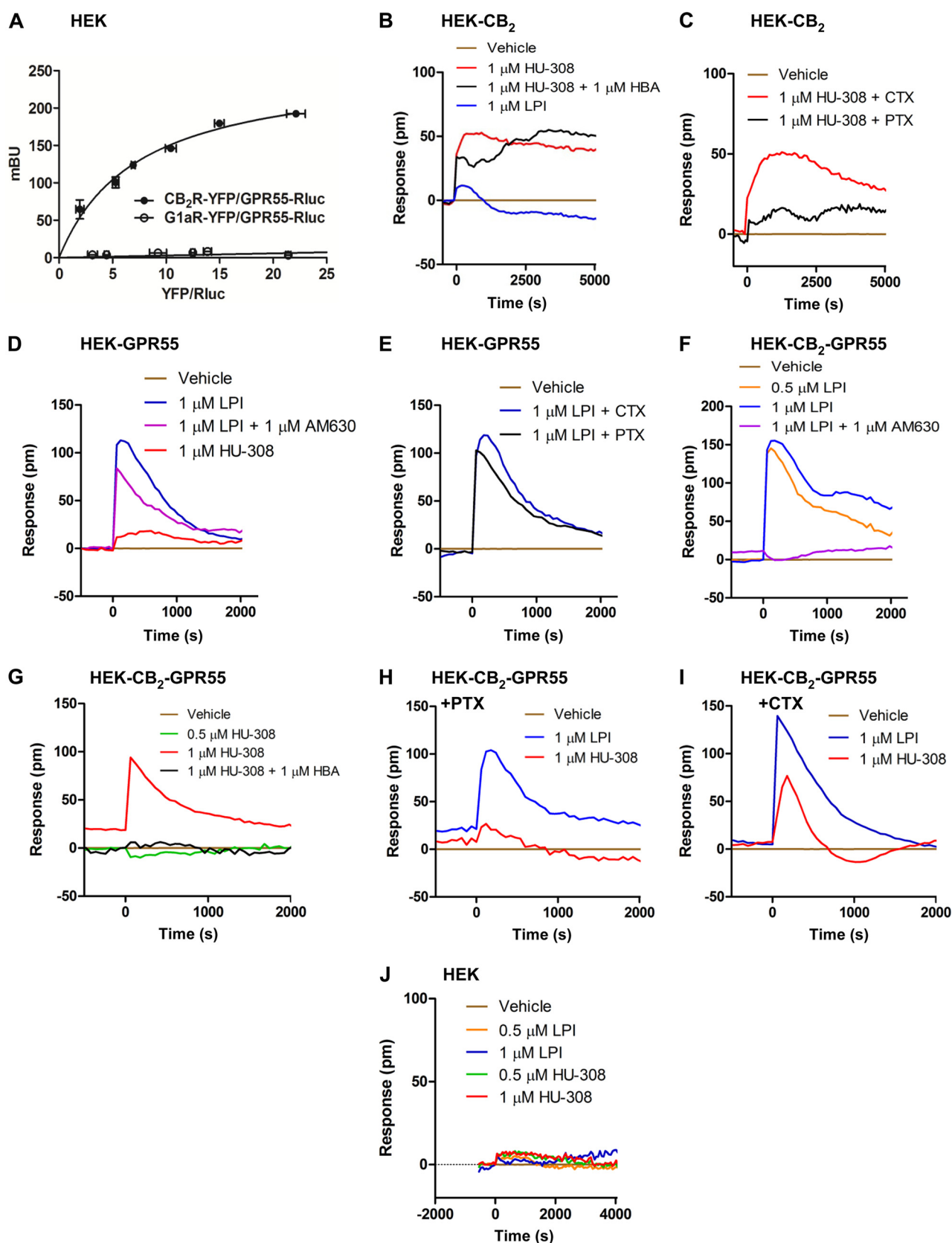


**FIGURE 1. Expression and functional characterization of CB<sub>2</sub>R-GPR55 heteromers in transfected HEK293 cells.** A, BRET saturation experiments were performed in cells transfected with a fixed amount of GPR55-Rluc cDNA (0.5  $\mu$ g) and increasing amounts (1–5  $\mu$ g) of CB<sub>2</sub>R-YFP or Ghrelin 1a receptor-YFP cDNAs. Values are the mean  $\pm$  S.E. of three to six different experiments grouped as a function of the amount of BRET acceptor. mBU, milliBRET unit. B–J, DMR in HEK-CB<sub>2</sub> (B and C), HEK-GPR55 (D and E), or HEK-CB<sub>2</sub>-GPR55 (F–I) cells not treated (B, D, F, and G) or treated overnight with 10 ng/ml PTX or with 100 ng/ml CTX prior to the addition of the antagonists HBA (B and G) or AM630 (D and F) and stimulation with LPI or HU-308. The resulting picometer (pm) shifts of reflected light wavelength versus time were monitored. Each curve is the mean of a representative optical trace experiment carried out in triplicates.

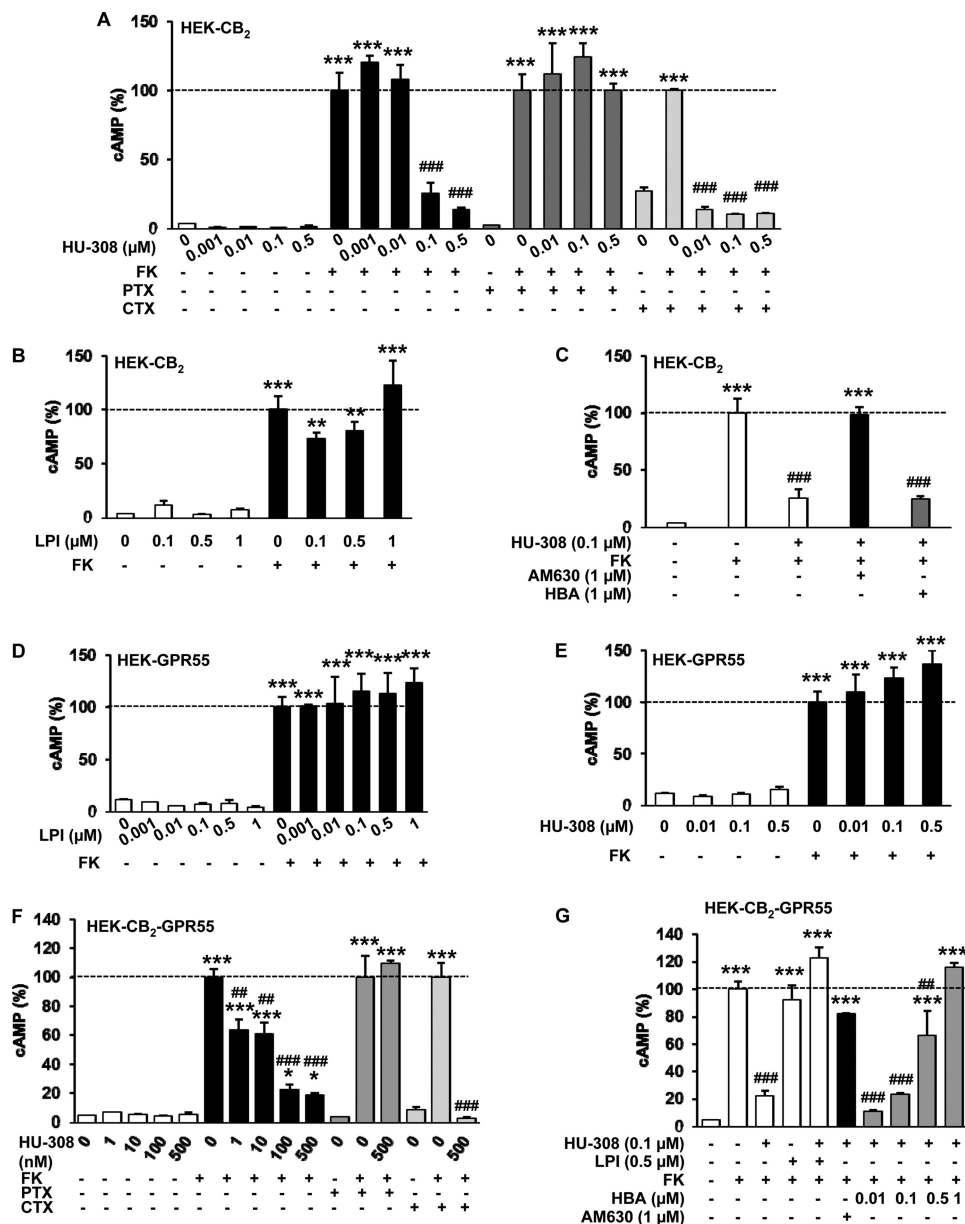


FIGURE 2. cAMP signaling in HEK293 cells expressing single receptors or CB<sub>2</sub>R-GPR55 heteromers. cAMP production in HEK-CB<sub>2</sub> (A–C), HEK-GPR55 (D and E), or HEK-CB<sub>2</sub>-GPR55 cells (F and G) treated (A and F) or not treated (B–E and G) overnight with 10 ng/ml PTX or with 100 ng/ml CTX. Cells were preincubated with vehicle or with the antagonists AM630 or HBA and stimulated with increasing concentrations of HU-308 or LPI in the absence or presence of 0.5 μM FK. Values are mean ± S.E. of *n* = 4–7 and are expressed as a percentage of the FK-treated cells in each condition. One-way ANOVA followed by Bonferroni post hoc test showed a significant effect over vehicle-treated cells (\*, *p* < 0.05; \*\*, *p* < 0.01; \*\*\*, *p* < 0.001) or over the FK effect (##, *p* < 0.01; ###, *p* < 0.001).

or 15 mg/kg/day) (The Health Concept) or the corresponding vehicle (PBS supplemented with 5% BSA) for 15 days. Tumors were measured routinely with external calipers, and the volume was calculated as  $(4\pi/3) \times (\text{width}/2)^2 \times (\text{length}/2)$ . At the end of the treatment, animals were sacrificed, and tumors were collected.

## RESULTS

**Expression and Functional Characterization of CB<sub>2</sub>R-GPR55 Heteromers in Transfected HEK293 Cells**—To analyze the possible molecular interaction between CB<sub>2</sub>R and GPR55, BRET experiments were performed. HEK293 cells expressing a fixed amount of GPR55-Rluc as the BRET donor and increasing amounts of CB<sub>2</sub>R-YFP as the BRET acceptor generated a hyper-

bolic and saturable BRET signal (Fig. 1A) with a BRET<sub>max</sub> of  $257 \pm 18$  milliBRET units and a BRET<sub>50</sub> of  $7.3 \pm 1.2$  that was not evident in cells expressing equivalent amounts of GPR55-Rluc and Ghrelin 1a receptor-YFP as a negative control (Fig. 1A). These results support that CB<sub>2</sub>R and GPR55 form heteromers in cotransfected cells.

We then analyzed whether the formation of these complexes alters the signaling properties of the individual protomers. To test which G proteins are coupled to the receptors when expressed alone, we used a label-free approach that measures DMR in the bottom 150 nm of a cell monolayer through detection of changes in light diffraction (23). In HEK293 cells expressing CB<sub>2</sub>R only (HEK-CB<sub>2</sub>), the CB<sub>2</sub>R-selective agonist

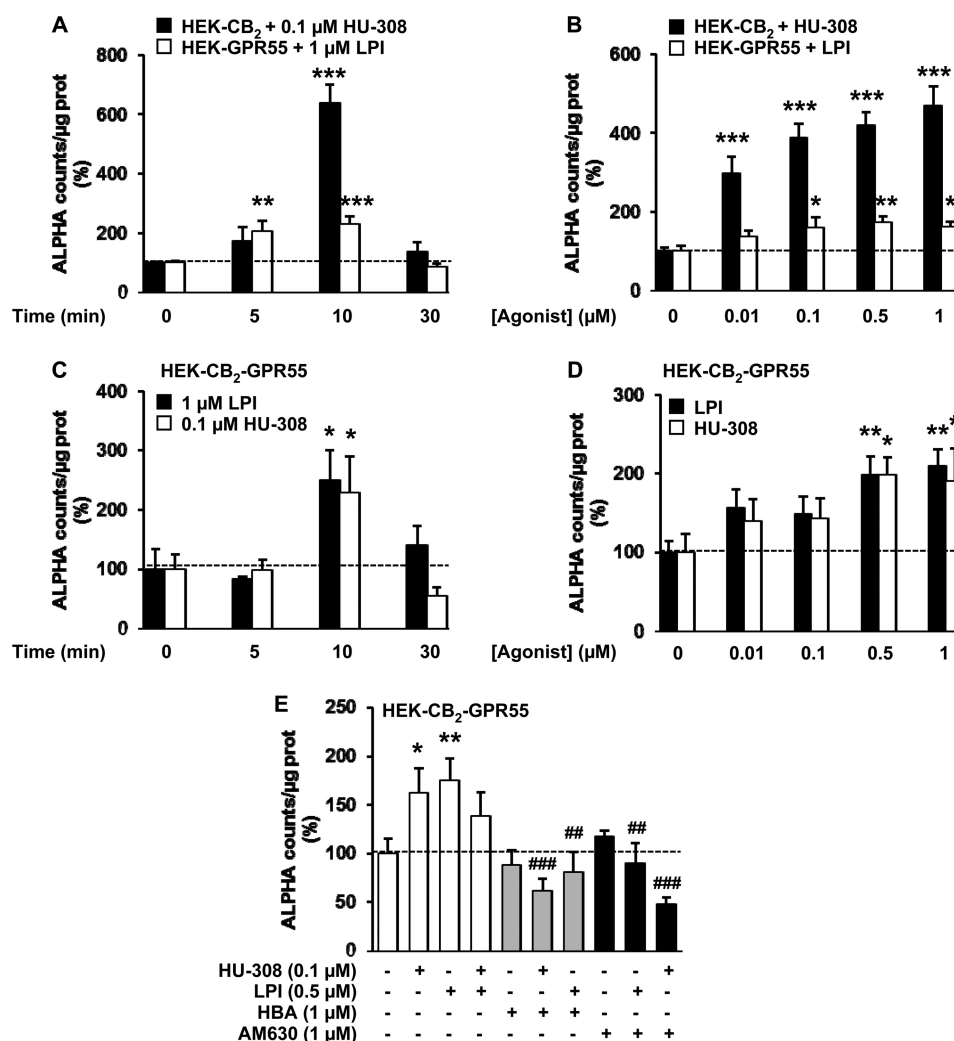


**FIGURE 3. ERK-1/2 phosphorylation in HEK293 cells expressing single receptors or CB<sub>2</sub>R-GPR55 heteromers.** A and B, ERK-1/2 phosphorylation was determined in HEK-CB<sub>2</sub> (black columns) or HEK-GPR55 (white columns) cells stimulated with 0.1 μM HU-308 or 1 μM LPI for different times (A) or for 7 min with increasing concentrations of HU-308 or LPI (B). C–E, ERK-1/2 phosphorylation was determined in HEK-CB<sub>2</sub>-GPR55 cells stimulated with 0.1 μM HU-308 or 1 μM LPI for different times (C), with increasing concentrations of these compounds for 7 min (D), or in cells pretreated with vehicle (white columns), with HBA (gray columns), or AM630 (black columns) prior to stimulation with HU-308, LPI, or both (E). Phosphorylation was expressed in arbitrary units (ALPHA counts, light emission at 520–620 nm). Values are mean ± S.E. of *n* = 6–9 and are expressed as a percentage over vehicle-treated cells. One-way ANOVA followed by Bonferroni post hoc test showed a significant effect over vehicle-treated cells (\*, *p* < 0.05; \*\*, *p* < 0.01; \*\*\*, *p* < 0.001) or of the antagonist plus agonist over the agonist treatment (E; ##, *p* < 0.01; ###, *p* < 0.001).

HU-308 produced a robust DMR signal (Fig. 1B) that was sensitive to pertussis toxin (PTX) but not to cholera toxin (CTX) (Fig. 1C). This is in line with many previous reports showing coupling of CB<sub>2</sub>R to G<sub>i</sub> heterotrimeric proteins (3). In HEK293 cells expressing GPR55 only (HEK-GPR55), we observed that the GPR55 agonist LPI produced a strong response (Fig. 1D) that was insensitive to CTX or PTX treatment (Fig. 1E), suggestive of coupling to G proteins other than G<sub>i</sub> and G<sub>s</sub>, as reported previously (8). Importantly, neither LPI nor HU-308 showed any activity in non-transfected cells (Fig. 1J), and both CB<sub>2</sub>R and GPR55 agonists and antagonists showed selectivity for their respective receptors with no agonist activation or antagonist blockade of the partner receptor in single receptor-expressing cells (Fig. 1, B and D). Interestingly, in HEK293 cells overexpressing both receptors (HEK-CB<sub>2</sub>-GPR55), we observed a similar coupling to G proteins but a different pharmacological behavior. In these cells, LPI induced a robust DMR signal (Fig. 1F) that was insensitive to CTX or PTX treatment

(Fig. 1, H and I), again suggesting coupling to G proteins different from G<sub>i</sub> and G<sub>s</sub>, and HU-308 induced a signal (Fig. 1G) that was blocked by PTX but not by CTX (Fig. 1, H and I), indicating a G<sub>i</sub> coupling. Surprisingly, the signal induced by LPI was completely blocked by the CB<sub>2</sub>R antagonist AM630 (Fig. 1F), and the signaling induced by HU-308 was blocked by the GPR55 antagonist 4-[4-(3-hydroxyphenyl)-3-(4-methylphenyl)-6-oxo-1H,4H,5H,6H-pyrrolo[3,4-c]pyrazol-5-yl] benzoic acid (HBA) (Fig. 1G). This cross-antagonism phenomenon suggests that, through the heteromer, one receptor can be targeted by using the partner receptor antagonist.

Because DMR experiments are indicative of global receptor signaling, we next investigated heteromer function in specific signaling pathways. In HEK-CB<sub>2</sub> cells, HU-308 (Fig. 2A), but not LPI (Fig. 2B), prevented the increase in cAMP levels elicited by forskolin (FK), an effect that was blocked by PTX but not by CTX (Fig. 2A) and by AM630 but not by HBA (Fig. 2C). In HEK-GPR55 cells, LPI produced no effect on FK-induced

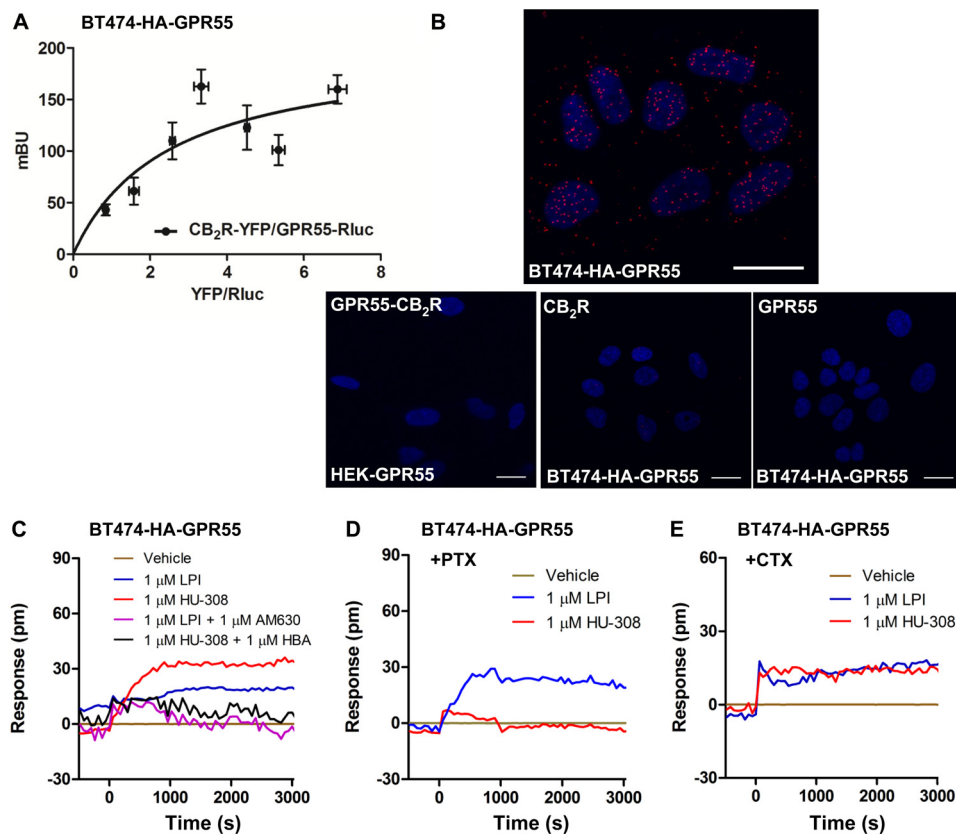


**FIGURE 4. Expression and functional characterization of CB<sub>2</sub>R-GPR55 heteromers in BT474 human breast cancer cells.** A, BRET saturation experiments were performed in BT474 cells transfected with 1  $\mu$ g of GPR55-Rluc cDNA and increasing amounts of CB<sub>2</sub>R-YFP cDNA (1–3  $\mu$ g). Values are given as the mean  $\pm$  S.E. of three to seven different experiments grouped as a function of the amount of BRET acceptor. mBU, milliBRET units. B, representative result of an *in situ* PLA performed in BT474-HA-GPR55 cells (upper panel). In the confocal microscopy image (superimposed sections) heteromers appear as red spots. Cell nuclei were stained with DAPI (blue). As negative controls (bottom panels), PLA were performed in HEK-GPR55 cells in the presence of anti-HA and anti-CB<sub>2</sub>R antibodies or in BT474-GPR55 cells in the absence of the anti-HA (CB<sub>2</sub>R) or the anti-CB<sub>2</sub>R antibodies (GPR55). Scale bars = 20  $\mu$ m. C–E, DMR analysis in BT474-HA-GPR55 cells not treated (C) or treated overnight with PTX (D, 10 ng/ml) or CTX (E, 100 ng/ml) prior to preincubation with the CB<sub>2</sub>R or the GPR55 antagonists (AM630 or HBA, respectively) and challenged with LPI or HU-308. The resulting picometer shifts of reflected light wavelength (picometer, pm) versus time were monitored. Each curve is the mean of a representative optical trace experiment carried out in triplicates.

cAMP levels (Fig. 2D), supporting coupling of this receptor to G proteins different from G<sub>i</sub> or G<sub>s</sub>. HU-308 did not induce any effect in these cells either (Fig. 2E). As observed in the label-free assays, HEK-CB<sub>2</sub>-GPR55 cells showed a different pharmacological behavior. HU-308 alone was still able to block the FK-induced cAMP increase through a PTX-sensitive mechanism (Fig. 1F). As expected in these cells, LPI was not able to increase or decrease (Fig. 1G) FK-stimulated cAMP levels. However, simultaneous activation of CB<sub>2</sub>R and GPR55 prevented HU-308 action (Fig. 1G), which is indicative of a negative cross-talk between both receptors. Moreover, in HEK-CB<sub>2</sub>-GPR55 cells, HU-308 effects on cAMP levels were blocked not only by AM630 but also by HBA (Fig. 1G). Similar negative cross-talk and cross-antagonism were detected in ERK-1/2 signaling. When expressed alone, activation of each receptor by its selective ligand resulted in a time- and dose-dependent increase in ERK-1/2 phosphorylation (Fig. 3, A and B). In cells expressing both receptors simultaneously, the activation of any of the protomers individually produced a similar response (Fig. 3, C and D). However, coactivation of both receptors resulted in reduced ERK-1/2 phosphorylation (Fig. 3E). In addition, LPI-induced ERK-1/2 phosphorylation was prevented by the CB<sub>2</sub>R antagonist, and HU-308 action was blocked by the GPR55

antagonist (*i.e.* cross-antagonist) (Fig. 3E). Together, these results support that CB<sub>2</sub>R and GPR55 form heteromers in cotransfected cells and that, via these complexes, agonists and antagonists of one receptor are able to impair the signaling of the partner receptor.

**Expression and Functional Characterization of CB<sub>2</sub>R-GPR55 Heteromers in Human Breast Cancer Cells**—Next we sought to determine whether CB<sub>2</sub>R-GPR55 heteromers are present in a more physiological setting, *i.e.* human cancer cells. First, BRET saturation curves performed in human breast adenocarcinoma BT474 cells transfected to express GPR55-Rluc and increasing amounts of CB<sub>2</sub>R-YFP indicated that these receptors also interact in cancer cells (Fig. 4A). This interaction was confirmed further by PLAs in BT474 cells endogenously expressing CB<sub>2</sub>R and stably expressing HA-GPR55 (BT474-GPR55). Heteromers were readily detectable in these cells (Fig. 4B, upper panel) but not in cells not expressing CB<sub>2</sub>R or upon removal of one of the primary antibodies (Fig. 4B, bottom panels). Of interest, the PLA-positive BT474 cells showed the same signaling profile as the aforementioned HEK-CB<sub>2</sub>-GPR55 cells. In label-free experiments, HU-308 induced a DMR signal that was sensitive to PTX and not to CTX, LPI induced a signal that was insensitive to toxins, and both LPI- and HU308-induced signals were



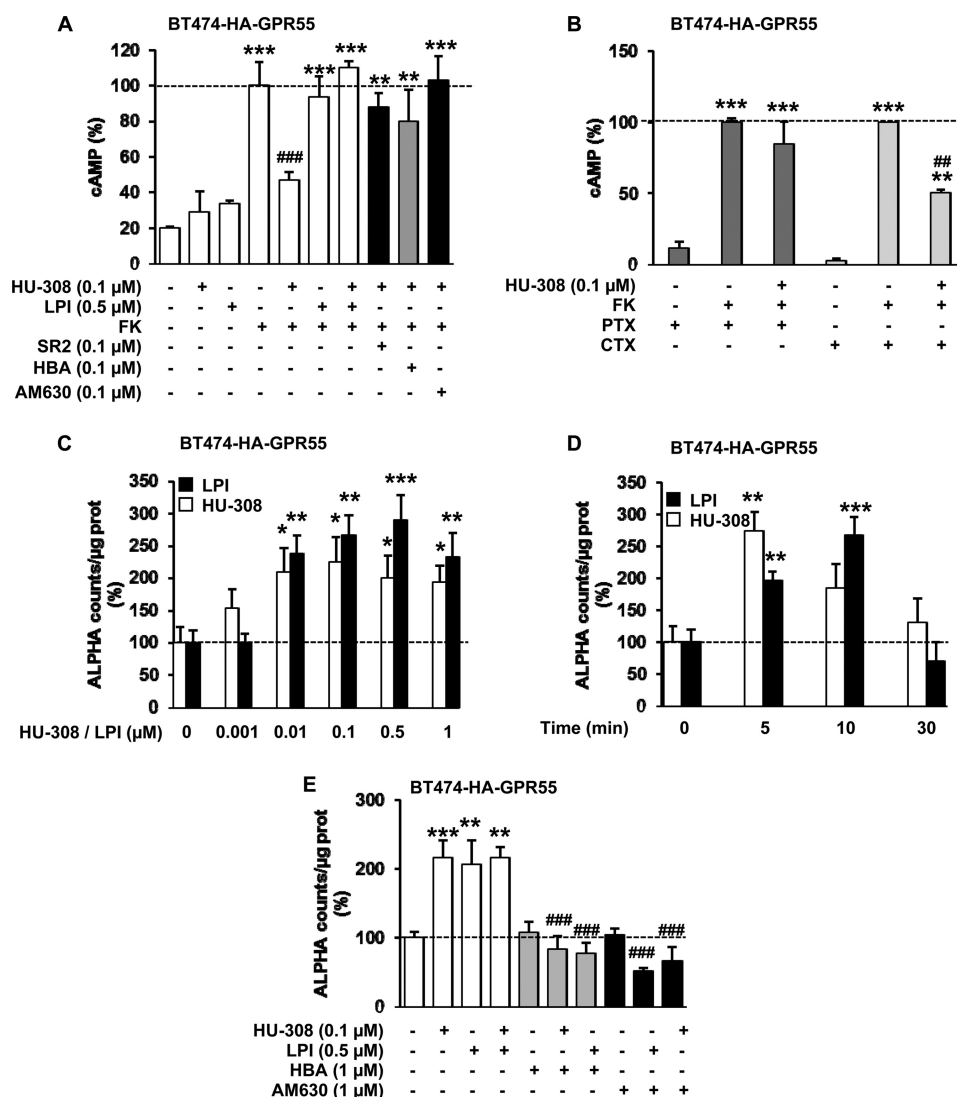


FIGURE 5. **cAMP production and ERK-1/2 phosphorylation mediated by CB<sub>2</sub>R-GPR55 heteromers in BT474 cancer cells.** A and B, cAMP production in BT474-GPR55 cells was determined in cells not pretreated (A) or pretreated overnight (B) with 10 ng/ml PTX or with 100 ng/ml CTX prior to incubation with the CB<sub>2</sub>R antagonists AM630 or SR144528 (SR2) or with the GPR55 antagonist HBA (A) and stimulated with HU-308, LPI, or both in the absence or in the presence of 0.5 μM FK. Values are mean ± S.E. of *n* = 3–9 and are expressed as a percentage of the FK-treated cells. C–E, ERK-1/2 phosphorylation was determined in BT474-GPR55 cells stimulated (7 min) with increasing concentrations of HU-308 or LPI (C), with 0.1 μM HU-308 or 1 μM LPI for different times (D), or pretreated or not treated with the CB<sub>2</sub>R antagonists AM630 or SR144528 or with the GPR55 antagonist HBA prior to stimulation with HU-308, LPI, or both (E). Phosphorylation was expressed in arbitrary units (ALPHA counts, light emission at 520–620 nm). Values are mean ± S.E. of *n* = 3–9 and are expressed as a percentage of basal levels found in vehicle-treated cells. One-way ANOVA followed by Bonferroni post hoc test showed a significant effect over vehicle-treated cells (\*\*\*, *p* < 0.001; \*\*, *p* < 0.01), over FK-treated cells (A and B; ##, *p* < 0.01; ###, *p* < 0.001), or antagonist plus agonist over the agonist treatment (E; ###, *p* < 0.001).

blocked by the antagonist of the partner receptor (Fig. 4, C–E). In addition, HU-308 (but not LPI) blocked the FK-induced cAMP increase (Fig. 5A), an effect that was sensitive to PTX but not to CTX (Fig. 5B). The HU308-induced effect was also prevented by coactivation with LPI (negative cross-talk) and not only by a CB<sub>2</sub>R antagonist but also by a GPR55 antagonist (cross-antagonism) (Fig. 5A). The negative cross-talk and cross-antagonism were also observed in the activation of ERK-1/2 (Fig. 5, C–E). Collectively, these findings support the existence of CB<sub>2</sub>R-GPR55 heteromers in cancer cells and show that these macromolecular structures have specific signaling properties.

**Differential Effects of THC in HEK293 Cells Expressing CB<sub>2</sub>R-GPR55 Heteromers or the Single Receptors**—Next, we analyzed the signaling response of HEK293 and cancer cells to the can-

nabinoid agonist THC. In agreement with previous observations (3), THC dose-dependently reduced FK-increased cAMP levels (Fig. 6A) and enhanced ERK-1/2 phosphorylation (Fig. 6B) in HEK-CB<sub>2</sub> cells. Interestingly, in HEK-CB<sub>2</sub>-GPR55 cells, a biphasic response was observed in both readouts. Although low concentrations of THC decreased FK-induced cAMP, higher THC concentrations attenuated this effect (Fig. 6C). Analogously, low concentrations of THC increased ERK-1/2 phosphorylation, whereas higher concentrations reduced this response (Fig. 6D). In support of the notion that these two-phase effects of THC are distinctive of the heteromers, we observed that the U-shaped curve in the cAMP assays (Fig. 6E) and the bell-shaped curve in the ERK-1/2 activation data (Fig. 6F) became flattened when cells were pretreated with either a CB<sub>2</sub>R or a GPR55 antagonist. From these observations, we



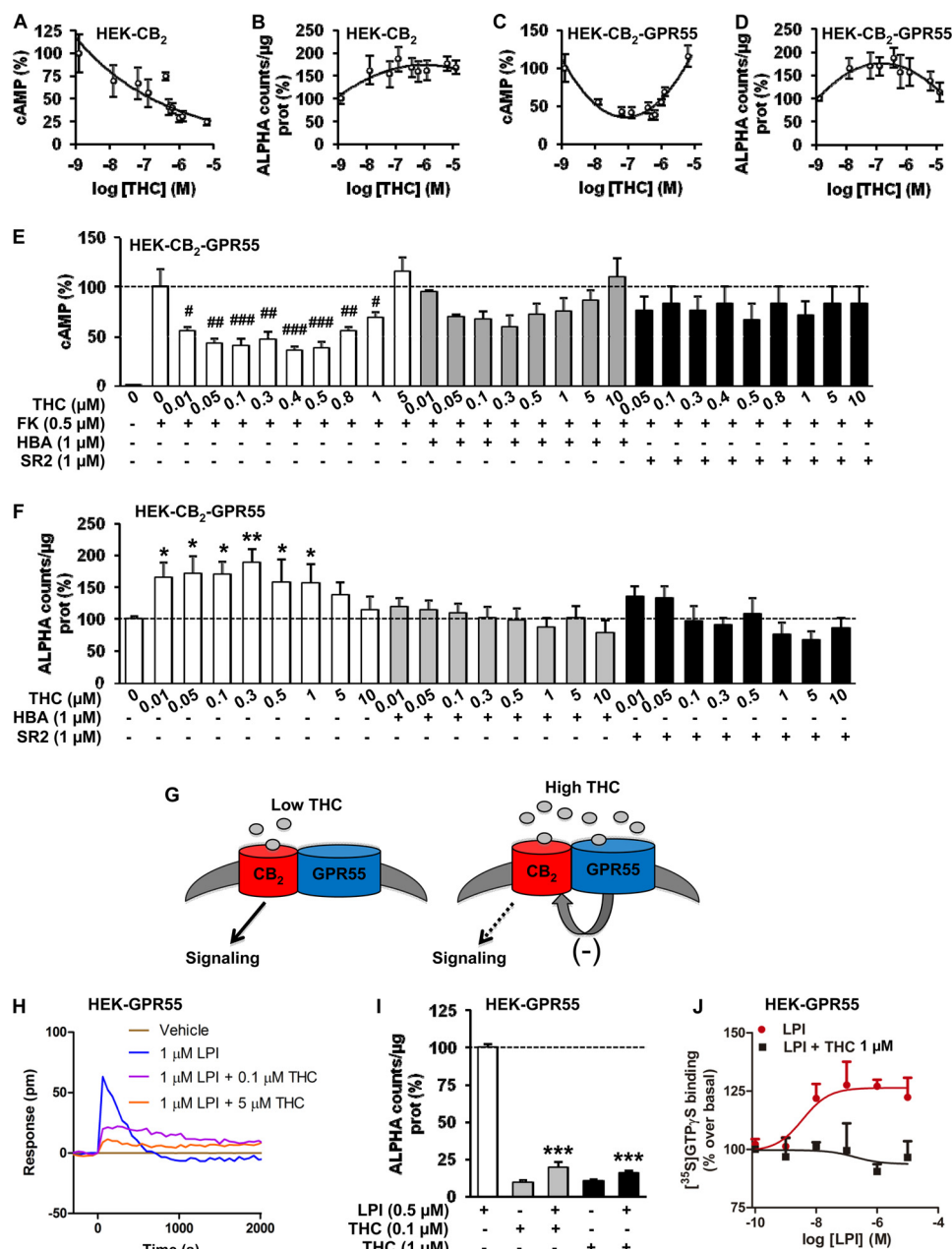


**FIGURE 6. Differential effects of THC in HEK293 cells expressing CB<sub>2</sub>R-GPR55 heteromers or the single receptors.** A–F, cAMP production in the absence or presence of FK (A, C, and E) and ERK-1/2 phosphorylation (B, D, and F) in response to increasing concentrations of THC in HEK-CB<sub>2</sub> (A and B) and HEK-CB<sub>2</sub>-GPR55 (C–F) cells. E and F, cells were pretreated with vehicle or the antagonists SR2 or HBA. Phosphorylation was expressed in arbitrary units (ALPHA counts, light emission at 520–620 nm). Values are mean ± S.E. of *n* = 5–12 and are expressed as a percentage of FK-treated cells (A, C, and E) or of vehicle-treated cells (B, D, and F). One-way ANOVA followed by Dunnett's post hoc test showed a significant effect over the effect of FK (E; #, *p* < 0.05; ##, *p* < 0.01; ###, *p* < 0.001) or over vehicle-treated cells (F; \*, *p* < 0.05; \*\*, *p* < 0.01). G, schematic of the hypothesized effect of THC on CB<sub>2</sub>R-GPR55 heteromers. At low concentrations, THC acts as a CB<sub>2</sub>R agonist promoting signaling. At higher concentrations, THC targets GPR55, acting as an antagonist. Via cross-antagonism through the heteromer, high THC concentrations inhibit CB<sub>2</sub>R signaling. H–J, DMR responses (H), ERK-1/2 phosphorylation (I), and GTPγS binding (J) in HEK-GPR55 cells in response to LPI and in the absence or presence of THC (J, 1 μM). H, the resulting picometer (pm) shifts of reflected light wavelength versus time were monitored. Each curve is the mean of a representative optical trace experiment carried out in triplicate. I, phosphorylation was expressed in arbitrary units (ALPHA counts, light emission at 520–620 nm). Values are mean ± S.E. of *n* = 4–6 and are expressed as a percentage relative to the effect of LPI. One-way ANOVA followed by Dunnett's post hoc tests showed a significant (\*\*\*, *p* < 0.001) effect over the LPI effect. J, [<sup>35</sup>S]GTPγS binding was expressed as the percentage over basal, and values are mean ± S.E. of *n* = 3, each one run in triplicate.

hypothesize the following mechanistic explanation for the biphasic action of THC (Fig. 6G). At low concentrations, THC (a well reported CB<sub>2</sub>R agonist) signals through CB<sub>2</sub>R, producing a conceivable activation of ERK-1/2 and inhibition of FK-induced cAMP increase (Fig. 6G). At higher concentrations, THC is able to target GPR55, acting as a receptor antagonist, as

suggested previously in Ref. 25, and exerting a cross-antagonism over CB<sub>2</sub>R through the heteromer, which would result in an attenuation of the CB<sub>2</sub>R-mediated effects on ERK-1/2 activation and cAMP production (Fig. 6G). In support of this idea, THC (which was not able to induce either DMR signals or ERK-1/2 phosphorylation in cells only expressing GPR55) decreased

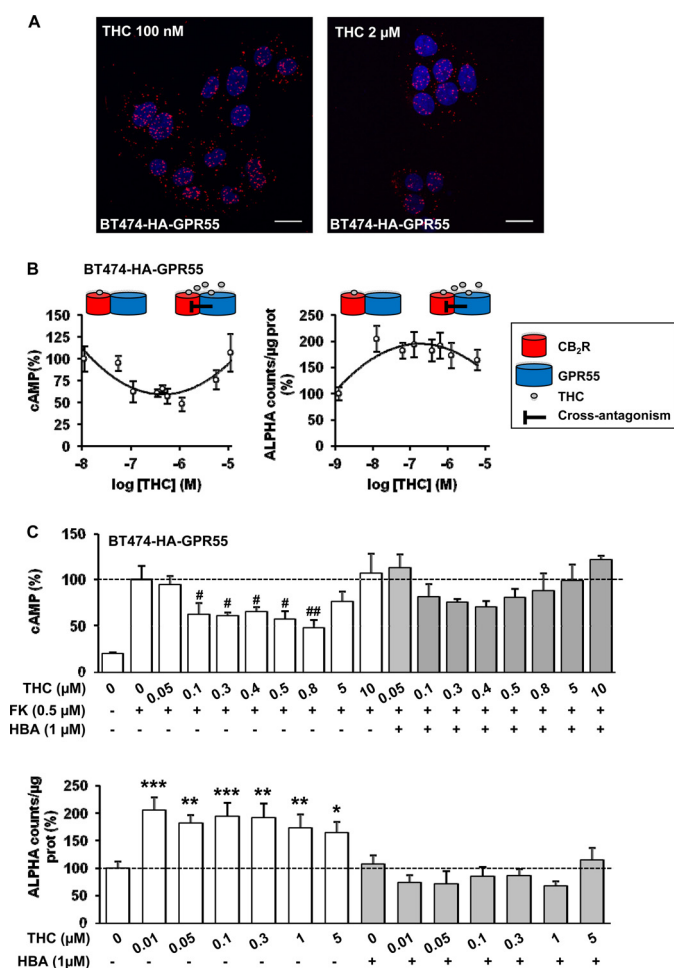


**FIGURE 7. Involvement of CB<sub>2</sub>R-GPR55 heteromers in the response of transfected cancer cells to THC.** *A*, representative results of *in situ* PLAs performed in BT474-HA-GPR55 cells treated (30 min) with high and low THC concentrations. In the confocal microscopy images (superimposed sections), heteromers appear as red spots. Cell nuclei were stained with DAPI (blue). Scale bars = 20 μm. *B*, the effect of THC on FK-induced cAMP production (left panel) and ERK-1/2 phosphorylation (right panel) in BT474-HA-GPR55 cells. Schematics depict the hypothesized THC mechanism of action. *C*, cAMP production (top panel) and ERK-1/2 phosphorylation (bottom panel) in BT474-GPR55 cells pretreated with vehicle or the GPR55 antagonist HBA prior to stimulation with THC. Top panel, cells were incubated in the absence or presence of 0.5 μM forskolin. Phosphorylation was expressed in arbitrary units (ALPHA counts, light emission at 520–620 nm). Values are mean ± S.E. of  $n = 5$ –12 and are expressed as a percentage of FK-treated cells (cAMP determination) or of vehicle-treated cells (ERK-1/2 phosphorylation). One-way ANOVA followed by Dunnett's post hoc test showed a significant effect over the effect of FK (#,  $p < 0.05$ ; ##,  $p < 0.01$ ) or over vehicle-treated cells ( $F$ ; \*,  $p < 0.05$ ; \*\*,  $p < 0.01$ ; \*\*\*,  $p < 0.001$ ).

LPI-induced DMR responses (Fig. 6H) and ERK-1/2 activation (Fig. 6I) in HEK-GPR55 cells. The capability of THC to prevent LPI-induced activation of GPR55 was further confirmed by GTPγS binding assays. LPI produced a marked increase in [<sup>35</sup>S]GTPγS binding in HEK-GPR55 membranes ( $E_{\max} = 129 \pm 2\%$ ;  $EC_{50} = 7.1 \pm 3.4$  nM), an effect that was completely blocked by coinubation with THC (Fig. 6J). Together, these results indicate that, at high concentrations, THC actually behaves as a GPR55 antagonist.

**Involvement of CB<sub>2</sub>R-GPR55 Heteromers in the Response of Cancer Cells to THC**—We then went back to cancer cells to challenge this hypothesis. First, PLA experiments showed that neither low nor high THC concentrations disrupt the CB<sub>2</sub>R-

GPR55 heteromers (Fig. 7A). Second, as in HEK-CB<sub>2</sub>-GPR55 cells, a two-phase effect of THC was observed in BT474-GPR55 cells on the modulation of both cAMP levels and ERK-1/2 phosphorylation, in which the response found at low concentrations was attenuated at higher concentrations (Fig. 7B). The U-shaped curve in the cAMP assays and the bell-shaped curve in the ERK-1/2 activation became less pronounced or even flattened when BT474-GPR55 cells were pretreated with the GPR55 antagonist HBA (Fig. 7C), demonstrating that the antagonistic effect of THC on GPR55 modulates CB<sub>2</sub>R signaling through CB<sub>2</sub>R-GPR55 heteromers.

Our hypothesis was further corroborated in T98G cells, a human glioblastoma cell line that endogenously expresses both CB<sub>2</sub>R (26) and GPR55 (12). By PLA, we detected red spots corresponding to CB<sub>2</sub>R-GPR55 heteromers (Fig. 8A, top left panel). Treatment of cells with either low or high concentrations of THC did not alter this staining (Fig. 8A, top panels), suggesting that the heteromers are not disrupted by the cannabinoid. The CB<sub>2</sub>R-GPR55 complexes were not detected in the negative controls, in which one of the primary antibodies was omitted, or in T98G cells, in which CB<sub>2</sub>R (T98G-shCB<sub>2</sub>) or GPR55 (T98G-shGPR55) expression was silenced (Fig. 8A, bottom panels). As in transfected cells, a two-phase effect of THC was observed in T98G cells on the modulation of both cAMP levels and ERK-1/2 phosphorylation, in which the response found at low concentrations was attenuated at higher concentrations (Fig. 8B). Finally, we analyzed the strength of our hypothesis in an *in vivo* setting. Subcutaneous tumors were generated by injection of T98G cells into athymic male mice. Tumors increased their growth slightly in response to a low THC dose (although no statistical differences were observed), whereas a higher THC dose produced the opposite effect, *i.e.* a significant reduction in tumor growth (Fig. 8C). According to our hypothesis, the low-dose effect would be produced mainly via activation of CB<sub>2</sub>R and the high-dose effect via cross-antagonism of CB<sub>2</sub>R upon targeting of GPR55. The direct antagonism of GPR55, a receptor that has been shown previously to drive tumorigenesis (12–14), by THC may contribute to this strong antitumoral response. Supporting the idea that GPR55 behaves as a tumor growth brake when targeted by high doses of THC, we observed that GPR55-silenced tumors increased their growth when exposed to THC (Fig. 8C). The differential effects of THC on tumor growth occurred in concert with differential changes in the levels of activated ERK-1/2, *i.e.* a reduction when CB<sub>2</sub>R and GPR55 were coexpressed and an enhancement when GPR55 was silenced (Fig. 8, D and E). These results support our hypothesis and suggest that the well established cannabinoid target CB<sub>2</sub>R, as well as GPR55, coparticipate, in part via direct receptor-receptor interaction, in the control of tumor growth in response to THC.

## DISCUSSION

The findings reported in this study lead to three important conclusions regarding the role of cannabinoids and their cognate receptors. First, we demonstrate the existence and function of CB<sub>2</sub>R-GPR55 heteromers in cancer cells. Second, we show that the expression of these receptor heteromers has a major impact on cannabinoid signaling in these cells. Finally,

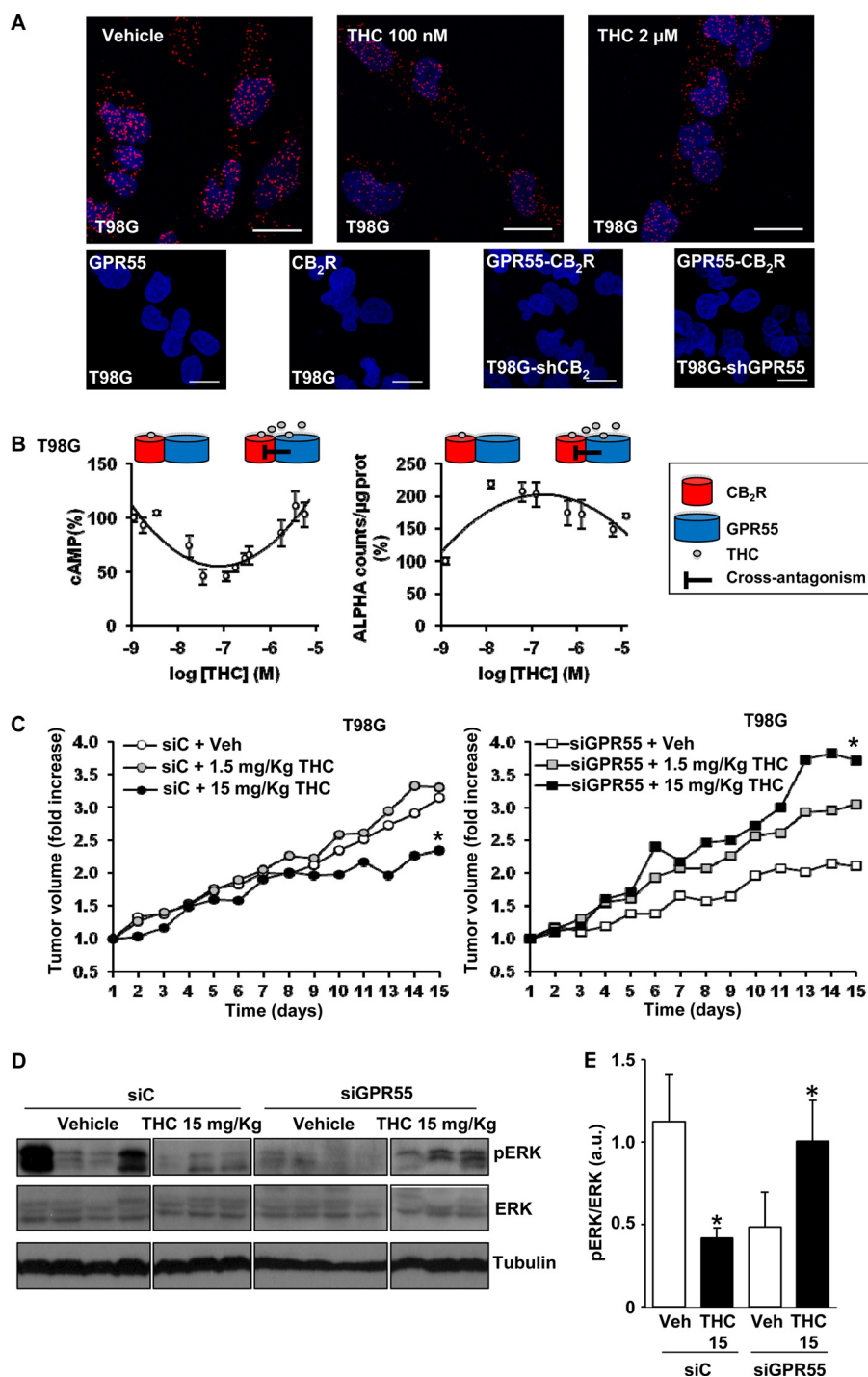


**FIGURE 8. Involvement of CB<sub>2</sub>R-GPR55 heteromers in the response to THC of cancer cells endogenously expressing CB<sub>2</sub>R and GPR55.** *A*, top panels, representative results of *in situ* PLAs performed in T98G cells treated (30 min) with vehicle and low and high THC concentrations. In the confocal microscopy images (*superimposed sections*), heteromers appear as *red spots*. Cell nuclei were stained with DAPI (*blue*). *Bottom panels*, as negative controls, PLAs were performed in T98G cells in the absence of anti-CB<sub>2</sub>R antibody (GPR55) or anti-GPR55 antibody (CB<sub>2</sub>R) or in the presence of anti-GPR55 and anti-CB<sub>2</sub>R antibodies in T98G cells in which CB<sub>2</sub>R (T98G-shCB<sub>2</sub>) or GPR55 (T98G-shGPR55) was silenced. Scale bars = 20  $\mu$ m. *B*, FK-induced cAMP production (*left panel*) and ERK-1/2 phosphorylation (*right panel*) in T98G cells in response to THC. Schematics depict the hypothesized THC mechanism of action. *C*, the volume of subcutaneous tumors generated by injection of T98G cells in immunodeficient mice was determined. Tumors were treated with a control siRNA (*left panel*) or a GPR55-selective siRNA (*right panel*), and animals received the indicated doses of THC or the corresponding vehicle (Veh). Tumor growth curves were compared by ANOVA with a post hoc analysis by Student-Newman-Keuls test. *D* and *E*, Western blot analysis (*D*) and densitometric analysis (*E*) of phospho-ERK-1/2 (pERK) in control siRNA (siC) and GPR55-siRNA tumors treated with 15 mg/Kg THC. \*,  $p < 0.05$  versus vehicle-treated animals (*C*) or cells (*E*).

our results suggest that direct targeting of CB<sub>2</sub>R-GPR55 via appropriate doses of THC may be an effective approach to reducing tumor growth.

Receptor heteromers involving the sister cannabinoid receptor CB<sub>1</sub> have been the focus of intense research. Therefore, CB<sub>1</sub>Rs have been shown previously to interact with other G



protein-coupled receptors, including dopamine D<sub>2</sub> receptors (which promotes a switch in the preferential coupling from G<sub>i</sub> to G<sub>s</sub>) (27), D<sub>2</sub> receptors and adenosine A<sub>2A</sub> receptors simultaneously (producing a negative modulation of D<sub>2</sub> receptor function by A<sub>2A</sub> and CB<sub>1</sub>R agonists) (28), opioid receptors (which produces a negative cross-talk between protomers) (29), orexin OX<sub>1</sub> receptors (eliciting a positive cross-talk in response to orexin and cross-antagonism) (30), and angiotensin AT<sub>1</sub> receptors (resulting in the potentiation of AT<sub>1</sub> receptor signaling) (31). More recently, coimmunoprecipitation assays in HEK293 cells have suggested that CB<sub>1</sub>R can form heteromers with GPR55 (32). In contrast to CB<sub>1</sub>R, very little is known about the possible existence and functional relevance of heteromers involving CB<sub>2</sub>R. A recent study has shown that CB<sub>2</sub>R heteromerizes with CB<sub>1</sub>R in neuronal cells in culture and *in vivo* (19). In these systems, coactivation of both receptors results in a negative cross-talk and a bidirectional cross-antagonism (19). However, CB<sub>2</sub>R signaling can be conceivably more relevant in non-differentiated cells, in which the receptor is highly abundant, than in terminally differentiated cells such as neurons, in which the receptor is scarce (3, 33). Specifically, CB<sub>2</sub>R, as well as GPR55, is notably overexpressed in a wide variety of cancer cell lines and human malignant tumors (6, 11), in which they play pivotal roles in controlling cancer cell fate (6, 11–14). It is tempting to speculate that CB<sub>2</sub>R-GPR55 heteromers may also exist and play pivotal signaling roles in other cells or tissues in which they are overexpressed, such as hematopoietic cells (16) or bones (34).

More and more studies have attempted to address the physiological role of GPR55. This receptor has been implicated in cancer, where it is generally linked with growth and proliferation (12–14). However, the molecular and cellular mechanisms behind these effects are still unanswered. In addition, it has been unclear whether GPR55's effects on proliferation involve CB<sub>2</sub>R or are independent. Considering the receptor heteromers discussed above and knowing that CB<sub>2</sub>R and GPR55 have been linked functionally in hematopoietic cells (16), we pursued the hypothesis that CB<sub>2</sub>R-GPR55 heteromers might play a role in the effects of GPR55 in cancer cells. Indeed, we found that these complexes were able to form in HEK293 cells and in both BT474 and T98G cancer cells and that they display a cross-talk and cross-antagonism at the level of the cAMP and p-ERK-1/2 pathways. We also found different cell signaling effects at low and high concentrations of THC and that this bimodal effect required the presence of the heteromer. Our findings that THC appears to be an antagonist of GPR55, at least at the level of cell signaling both of the single receptor and within the CB<sub>2</sub>R-GPR55 heteromer, were particularly surprising. Previous reports have indeed suggested this (25), and the data we obtained in three different cell lines as well as in a mouse model of cancer *in vivo* support these conclusions. This is in line with the general idea that, despite the potential relationship between cannabinoid receptors and GPR55, their pharmacology is very different (8, 35).

Finally, our discovery that CB<sub>2</sub>R-GPR55 complexes have unique pharmacological and signaling properties and are critically involved in the response of cancer cells to THC both *in vitro* and *in vivo* opens new doors to the development of com-

pounds targeting these heteromers as novel sites of intervention for future cancer studies. Our results also shed light on the possible molecular mechanisms underlying the well known but still poorly understood biphasic effects of cannabinoids, which have been reported for several decades regarding their action on food intake, motor behavior, and anxiety, among others (36–38).

*Acknowledgments*—We thank Dr. Nariman Balenga and Dr. Julia Kargl for generation of the HEK cell lines.

## REFERENCES

- Dorsam, R. T., and Gutkind, J. S. (2007) G-protein-coupled receptors and cancer. *Nat. Rev. Cancer* **7**, 79–94
- Rosenbaum, D. M., Rasmussen, S. G., and Kobilka, B. K. (2009) The structure and function of G-protein-coupled receptors. *Nature* **459**, 356–363
- Pertwee, R. G., Howlett, A. C., Abood, M. E., Alexander, S. P., Di Marzo, V., Elphick, M. R., Greasley, P. J., Hansen, H. S., Kunos, G., Mackie, K., Mechoulam, R., and Ross, R. A. (2010) International Union of Basic and Clinical Pharmacology: LXXIX: cannabinoid receptors and their ligands: beyond CB and CB. *Pharmacol. Rev.* **62**, 588–631
- Pacher, P., Bátkai, S., and Kunos, G. (2006) The endocannabinoid system as an emerging target of pharmacotherapy. *Pharmacol. Rev.* **58**, 389–462
- Guzmán, M., Sánchez, C., and Galve-Roperh, I. (2002) Cannabinoids and cell fate. *Pharmacol. Ther.* **95**, 175–184
- Velasco, G., Sánchez, C., and Guzmán, M. (2012) Towards the use of cannabinoids as antitumour agents. *Nat. Rev. Cancer* **12**, 436–444
- Brown, A. J. (2007) Novel cannabinoid receptors. *Br. J. Pharmacol.* **152**, 567–575
- Ross, R. A. (2009) The enigmatic pharmacology of GPR55. *Trends Pharmacol. Sci.* **30**, 156–163
- Oka, S., Nakajima, K., Yamashita, A., Kishimoto, S., and Sugiura, T. (2007) Identification of GPR55 as a lysophosphatidylinositol receptor. *Biochem. Biophys. Res. Commun.* **362**, 928–934
- Pertwee, R. G. (2010) Receptors and channels targeted by synthetic cannabinoid receptor agonists and antagonists. *Curr. Med. Chem.* **17**, 1360–1381
- Henstridge, C. M., Balenga, N. A., Kargl, J., Andradas, C., Brown, A. J., Irving, A., Sanchez, C., and Waldhoer, M. (2011) Minireview: recent developments in the physiology and pathology of the lysophosphatidylinositol-sensitive receptor GPR55. *Mol. Endocrinol.* **25**, 1835–1848
- Andradas, C., Caffarel, M. M., Pérez-Gómez, E., Salazar, M., Lorente, M., Velasco, G., Guzmán, M., and Sánchez, C. (2011) The orphan G protein-coupled receptor GPR55 promotes cancer cell proliferation via ERK. *Oncogene* **30**, 245–252
- Pérez-Gómez, E., Andradas, C., Flores, J. M., Quintanilla, M., Paramio, J. M., Guzmán, M., and Sánchez, C. (2013) The orphan receptor GPR55 drives skin carcinogenesis and is upregulated in human squamous cell carcinomas. *Oncogene* **32**, 2534–2542
- Piñeiro, R., Maffucci, T., and Falasca, M. (2011) The putative cannabinoid receptor GPR55 defines a novel autocrine loop in cancer cell proliferation. *Oncogene* **30**, 142–152
- Rozenfeld, R., and Devi, L. A. (2010) Receptor heteromerization and drug discovery. *Trends Pharmacol. Sci.* **31**, 124–130
- Balenga, N. A., Aflaki, E., Kargl, J., Platzer, W., Schröder, R., Blättermann, S., Kostenis, E., Brown, A. J., Heinemann, A., and Waldhoer, M. (2011) GPR55 regulates cannabinoid 2 receptor-mediated responses in human neutrophils. *Cell Res.* **21**, 1452–1469
- Henstridge, C. M., Balenga, N. A., Ford, L. A., Ross, R. A., Waldhoer, M., and Irving, A. J. (2009) The GPR55 ligand 1- $\alpha$ -lysophosphatidylinositol promotes RhoA-dependent Ca<sup>2+</sup> signaling and NFAT activation. *FASEB J.* **23**, 183–193
- González, S., Rangel-Barajas, C., Peper, M., Lorenzo, R., Moreno, E., Ciruela, F., Borycz, J., Ortiz, J., Lluís, C., Franco, R., McCormick, P. J., Volkow, N. D., Rubinstein, M., Floran, B., and Ferré, S. (2012) Dopamine D4 recep-



- tor, but not the ADHD-associated D4.7 variant, forms functional heteromers with the dopamine D2S receptor in the brain. *Mol. Psychiatry* **17**, 650–662
19. Callén, L., Moreno, E., Barroso-Chinea, P., Moreno-Delgado, D., Cortés, A., Mallol, J., Casadó, V., Lanciego, J. L., Franco, R., Lluís, C., Canela, E. I., and McCormick, P. J. (2012) Cannabinoid receptors CB1 and CB2 form functional heteromers in brain. *J. Biol. Chem.* **287**, 20851–20865
20. Carriba, P., Navarro, G., Ciruela, F., Ferré, S., Casadó, V., Agnati, L., Cortés, A., Mallol, J., Fuxe, K., Canela, E. I., Lluís, C., and Franco, R. (2008) Detection of heteromerization of more than two proteins by sequential BRET-FRET. *Nat. Methods* **5**, 727–733
21. Söderberg, O., Leuchowius, K. J., Gullberg, M., Jarvius, M., Weibrecht, L., Larsson, L. G., and Landegren, U. (2008) Characterizing proteins and their interactions in cells and tissues using the in situ proximity ligation assay. *Methods* **45**, 227–232
22. Trifilieff, P., Rives, M. L., Urizar, E., Piskrowski, R. A., Vishwasrao, H. D., Castrillon, J., Schmauss, C., Slättman, M., Gullberg, M., and Javitch, J. A. (2011) Detection of antigen interactions *ex vivo* by proximity ligation assay: endogenous dopamine D2-adenosine A2A receptor complexes in the striatum. *BioTechniques* **51**, 111–118
23. Schröder, R., Janssen, N., Schmidt, J., Kebig, A., Merten, N., Hennen, S., Müller, A., Blättermann, S., Mohr-Andrä, M., Zahn, S., Wenzel, J., Smith, N. J., Gomez, J., Drewke, C., Milligan, G., Mohr, K., and Kostenis, E. (2010) Deconvolution of complex G protein-coupled receptor signaling in live cells using dynamic mass redistribution measurements. *Nat. Biotechnol.* **28**, 943–949
24. Mato, S., Vidal, R., Castro, E., Díaz, A., Pazos, A., and Valdizán, E. M. (2010) Long-term fluoxetine treatment modulates cannabinoid type 1 receptor-mediated inhibition of adenylyl cyclase in the rat prefrontal cortex through 5-hydroxytryptamine 1A receptor-dependent mechanisms. *Mol. Pharmacol.* **77**, 424–434
25. Anavi-Goffer, S., Baillie, G., Irving, A. J., Gertsch, J., Greig, I. R., Pertwee, R. G., and Ross, R. A. (2012) Modulation of L- $\alpha$ -lysophosphatidylinositol/GPR55 mitogen-activated protein kinase (MAPK) signaling by cannabinoids. *J. Biol. Chem.* **287**, 91–104
26. Lorente, M., Torres, S., Salazar, M., Carracedo, A., Hernández-Tiedra, S., Rodríguez-Fornés, F., García-Taboada, E., Meléndez, B., Mollejo, M., Campos-Martín, Y., Lakatos, S. A., Barcia, J., Guzmán, M., and Velasco, G. (2011) Stimulation of the midkine/ALK axis renders glioma cells resistant to cannabinoid antitumoral action. *Cell Death Differ.* **18**, 959–973
27. Marcellino, S., Attar, H., Lièvremon, D., Lett, M. C., Barbier, F., and Lagarde, F. (2008) Heat-treated *Saccharomyces cerevisiae* for antimony speciation and antimony(III) preconcentration in water samples. *Anal. Chim. Acta* **629**, 73–83
28. Navarro, G., Ferré, S., Cordomi, A., Moreno, E., Mallol, J., Casadó, V., Cortés, A., Hoffmann, H., Ortiz, J., Canela, E. I., Lluís, C., Pardo, L., Franco, R., and Woods, A. S. (2010) Interactions between intracellular domains as key determinants of the quaternary structure and function of receptor heteromers. *J. Biol. Chem.* **285**, 27346–27359
29. Rios, C., Gomes, I., and Devi, L. A. (2006)  $\mu$  Opioid and CB1 cannabinoid receptor interactions: reciprocal inhibition of receptor signaling and neurogenesis. *Br. J. Pharmacol.* **148**, 387–395
30. Ellis, J., Pediani, J. D., Canals, M., Milasta, S., and Milligan, G. (2006) Orexin-1 receptor-cannabinoid CB1 receptor heterodimerization results in both ligand-dependent and -independent coordinated alterations of receptor localization and function. *J. Biol. Chem.* **281**, 38812–38824
31. Rozenfeld, R., Gupta, A., Gagnidze, K., Lim, M. P., Gomes, I., Lee-Ramos, D., Nieto, N., and Devi, L. A. (2011) AT1R-CB(1)R heteromerization reveals a new mechanism for the pathogenic properties of angiotensin II. *EMBO J.* **30**, 2350–2363
32. Kargl, J., Balenga, N., Parzmair, G. P., Brown, A. J., Heinemann, A., and Waldhoer, M. (2012) The cannabinoid receptor CB1 modulates the signaling properties of the lysophosphatidylinositol receptor GPR55. *J. Biol. Chem.* **287**, 44234–44248
33. Pertwee, R. G. (2009) Emerging strategies for exploiting cannabinoid receptor agonists as medicines. *Br. J. Pharmacol.* **156**, 397–411
34. Whyte, L. S., Ryberg, E., Sims, N. A., Ridge, S. A., Mackie, K., Greasley, P. J., Ross, R. A., and Rogers, M. J. (2009) The putative cannabinoid receptor GPR55 affects osteoclast function *in vitro* and bone mass *in vivo*. *Proc. Natl. Acad. Sci. U.S.A.* **106**, 16511–16516
35. Rempel, V., Volz, N., Gläser, F., Nieger, M., Bräse, S., and Müller, C. E. (2013) Antagonists for the orphan G-protein-coupled receptor GPR55 based on a coumarin scaffold. *J. Med. Chem.* **56**, 4798–4810
36. Moreira, F. A., and Wotjak, C. T. (2010) Cannabinoids and anxiety. *Curr. Top. Behav. Neurosci.* **2**, 429–450
37. Sañudo-Peña, M. C., Romero, J., Seale, G. E., Fernandez-Ruiz, J. J., and Walker, J. M. (2000) Activational role of cannabinoids on movement. *Eur. J. Pharmacol.* **391**, 269–274
38. Sulcova, E., Mechoulam, R., and Fride, E. (1998) Biphasic effects of anandamide. *Pharmacol. Biochem. Behav.* **59**, 347–352

## Targeting CB<sub>2</sub>-GPR55 Receptor Heteromers Modulates Cancer Cell Signaling

Estefanía Moreno, Clara Andradás, Mireia Medrano, María M. Caffarel, Eduardo Pérez-Gómez, Sandra Blasco-Benito, María Gómez-Cañas, M. Ruth Pazos, Andrew J. Irving, Carme Lluís, Enric I. Canela, Javier Fernández-Ruiz, Manuel Guzmán, Peter J. McCormick and Cristina Sánchez

*J. Biol. Chem.* 2014, 289:21960-21972.

doi: 10.1074/jbc.M114.561761 originally published online June 18, 2014

---

Access the most updated version of this article at doi: [10.1074/jbc.M114.561761](https://doi.org/10.1074/jbc.M114.561761)

### Alerts:

- [When this article is cited](#)
- [When a correction for this article is posted](#)

[Click here](#) to choose from all of JBC's e-mail alerts

This article cites 38 references, 11 of which can be accessed free at <http://www.jbc.org/content/289/32/21960.full.html#ref-list-1>